Impact of tricuspid annuloplasty device shape and size on valve mechanics—a computational study

Collin E. Haese, MS,[a] Mrudang Mathur, BTech,[b] Chien-Yu Lin, MS,[c] Marcin Malinowski, MD, PhD,[d,e] Tomasz A. Timek, MD, PhD,[e] and Manuel K. Rausch, PhD[a,b,c]

ABSTRACT

Background: Tricuspid valve disease significantly affects 1.6 million Americans. The gold standard treatment for tricuspid disease is the implantation of annuloplasty devices. These ring-like devices come in various shapes and sizes. Choices for both shape and size are most often made by surgical intuition rather than scientific rationale.

Methods: To understand the impact of shape and size on valve mechanics and to provide a rational basis for their selection, we used a subject-specific finite element model to conduct a virtual case study. That is, we implanted 4 different annuloplasty devices of 6 different sizes in our virtual patient. After each virtual surgery, we computed the coaptation area, leaflet end-systolic angles, leaflet stress, and chordal forces.

Results: We found that contoured devices are better at normalizing end-systolic angles, whereas the one flat device, the Edwards Classic, maximized the coaptation area and minimized leaflet stress and chordal forces. We further found that reducing device size led to increased coaptation area but also negatively impacted end-systolic angles, stress, and chordal forces.

Conclusions: Based on our analyses of the coaptation area, leaflet motion, leaflet stress, and chordal forces, we found that device shape and size have a significant impact on valve mechanics. Thereby, our study also demonstrates the value of simulation tools and device tests in "virtual patients." Expanding our study to many more valves may, in the future, allow for universal recommendations. (JTCVS Open 2024;17:111-20)

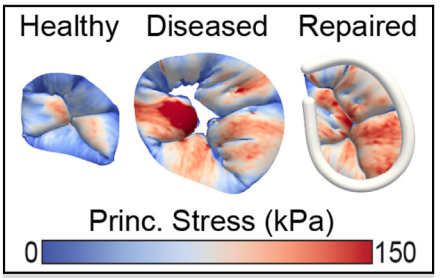

Atrial view of the healthy, diseased, and one of the 24 virtually repaired tricuspid valves.

CENTRAL MESSAGE

The choice of annuloplasty device shape and size used to treat tricuspid regurgitation significantly affects valve mechanics; namely, coaptation area, chordal forces, and leaflet motion and stress.

PERSPECTIVE

Annuloplasty remains the primary surgical treatment of tricuspid valve regurgitation. We virtually repaired a patient using 4 different device shapes of 6 sizes each to investigate the role of device choice in valve repair. We found that contoured devices are better at returning healthy valve kinematics whereas the flat device maximized leaflet coaptation and minimized leaflet stress.

From the [a]Department of Aerospace Engineering and Engineering Mechanics, [b]Walker Department of Mechanical Engineering, and [c]Department of Biomedical Engineering, The University of Texas at Austin, Austin, Tex; [d]Department of Cardiac Surgery, Medical University of Silesia, Katowice, Poland; and [e]Division of Cardiothoracic Surgery, Spectrum Health, Grand Rapids, Mich.

This work was supported by grants of the American Heart Association to M.Mat. (902502) and M.K.R. (18CDA34120028), as well as the National Institutes of Health through awards to M.K.R. and T.A.T. (1R21HL161832 and 1R01HL165251). The authors acknowledge the Texas Advanced Computing Center (TACC) at The University of Texas at Austin for providing high-performance computing resources that have contributed to the research results reported within this paper.

Received for publication Sept 20, 2023; revisions received Oct 28, 2023; accepted for publication Oct 31, 2023; available ahead of print Dec 12, 2023.

Address for reprints: Manuel K. Rausch, PhD, Department of Aerospace Engineering and Engineering Mechanics, The University of Texas at Austin, 2617 Wichita St, North Office Building A, Austin, TX 78712 (E-mail: manuel.rausch@utexas.edu).

2666-2736

https://doi.org/10.1016/j.xjon.2023.11.002

An estimated 1.6 million Americans suffer significantly from tricuspid valve regurgitation.[1] Valve failure is most often secondary to other conditions.[2,3] That is, outward remodeling and dilation of the right ventricle increase the tricuspid valve circumference and pull on the valve's chordal structure.[3,4] Together, these mechanisms alter valve mechanics and thus disrupt its leaflets' ability to coapt.

When leakage is severe, valve repair is required, for which surgical annuloplasty remains the gold standard.[5] During this procedure, a ring-like device is implanted with the intent of restoring the healthy tricuspid annular shape and leaflet coaptation.[6] Today, surgeons can choose from a range of devices that come in different shapes and sizes.[7] Although manufacturers provide guidelines for choosing device type (ie, shape) and size, device selection is often driven by surgeon experience and preference. For example, one documented strategy is to choose the device size identically to the device size chosen for the concomitant mitral valve repair.[8,9] Others choose to always pick the smallest available size.[10,11] The variability in device selection strategies and the clear lack of objective guidelines may explain, at least in part, why regurgitation recurs in 10% to 30% of patients within a few years of surgery.[6,12,13] Thus, objective guidelines may improve surgical outcomes. Toward such guidelines, we first must understand the impact of device shape and size on tricuspid valve mechanics.

The impact of device selection on valve mechanics is mostly unknown, which stems from (1) our inability to directly compare different devices within a single patient and (2) direct comparison of the repaired valve with the original, healthy valve being obviously impossible in a clinical setting. Computational models can overcome these clinical limitations by providing access to both the healthy and the diseased valve and by allowing for a direct comparison between different devices. Thus, to study the impact of annuloplasty device shape and size on tricuspid valve function, our goal is to use our previously developed and validated Texas TriValve 1.0 as a case study in which we virtually implant and compare four different devices in six sizes.

METHODS

Texas TriValve Disease Model

For this work, we used the Texas TriValve 1.0. A complete account of all model details, including the geometry, material properties, and boundary conditions, can be found in Appendix E1 and our recent work.[14] To investigate the impact of device shape and size on the mechanics of the diseased, ie, regurgitant, tricuspid valve, we altered our published healthy valve model to mirror the pathology of pulmonary arterial hypertension-induced functional tricuspid regurgitation. As such, we asymmetrically dilated the tricuspid annulus in the lateral direction until achieving an end-diastolic annular area increase of 62% and an annular circularity of one.[15] The free edges of the leaflets were passively dilated by the same amount, thus retaining their original leaflet height but increasing their surface area by approximately 30%, similar to values seen in Meador and colleagues.[16] We also held the thickness of the leaflets constant while we displaced the papillary muscle heads to induce tethering of the chordae tendineae.[17] Finally, we increased the transvalvular pressure load to 42.5 mm Hg to account for our virtual patient's hypertensive state[18] (Figure 1).

Virtual Device Implantation

In total, we virtually implanted 24 annuloplasty devices, 4 different shapes of 6 different sizes (26 to 36). Three devices were chosen from Edwards Lifesciences' offering, the Cosgrove-Edwards Classic Ring model 4500 (Classic), the Carpentier-Edwards Physio Tricuspid Ring model 6200 (Physio), and the Edwards MC3 Tricuspid Ring model 4900 (MC3); and one device was from Medtronic's offering, the Contour 3D Ring model 690R (Contour). Figure 2 shows all 4 annuloplasty devices used in this study. Note all devices are considered "rigid" or "stiff."[19] The exact geometries of the devices were determined via 3D scanning[20]; device areas and heights are provided in Table 1. The virtual repairs themselves were conducted using Abaqus/Explicit, in which we simulated first the device implantation and then the post-repair valve closure. Simulation details are provided in Appendix E2.

RESULTS

Leaflet Coaptation

Figure 3 shows the outcomes of all 24 virtual repairs. We first found that not all device shape and size combinations restored full leaflet coaptation. For those shape and size

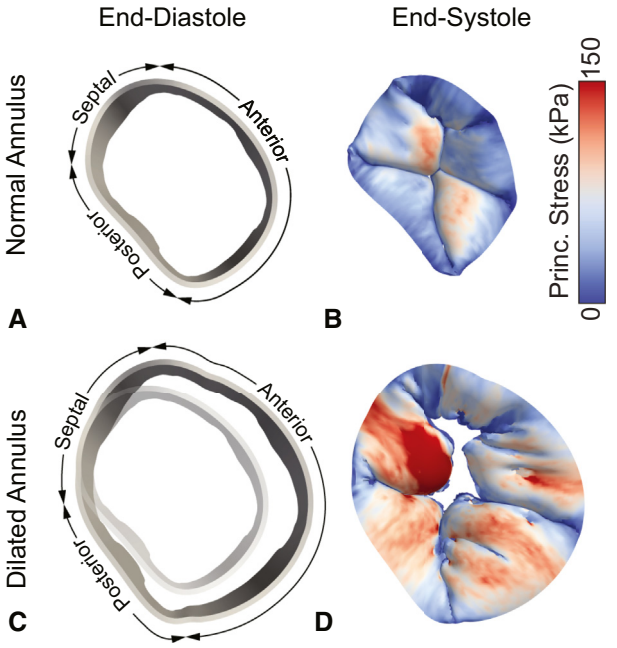

FIGURE 1. Atrial view of the Texas TriValve 1.0 at end-diastole and end-systole. Healthy Texas TriValve with a normal annulus in the (A) open, end-diastolic configuration and (B) closed, end-systolic configuration. Diseased Texas TriValve with a dilated annulus in the (C) open, end-diastolic configuration and (D) closed, end-systolic configuration; overlaid with contours of maximum principal Cauchy stress.

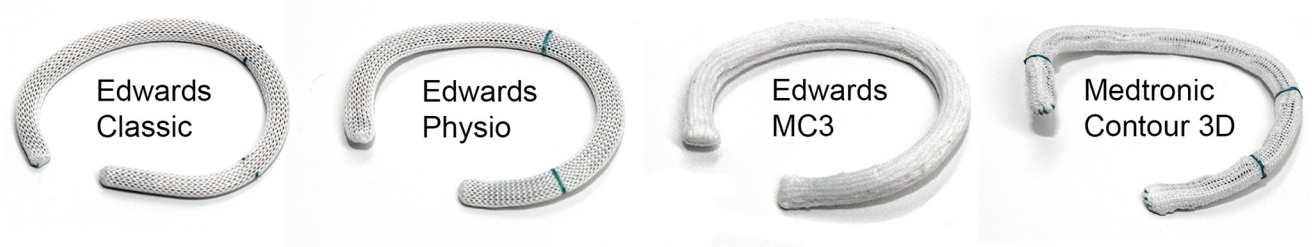

FIGURE 2. The 4 different annuloplasty devices used in this study. Three devices were from Edwards Lifesciences, the Cosgrove-Edwards Classic Ring (Classic), the Carpentier-Edwards Physio Tricuspid Ring (Physio), and the Edwards MC3 Tricuspid Ring (MC3); and one device was from Medtronic, the Contour 3D Ring (Contour). Reproduced with permission from Mathur and colleagues.[20]

combinations that failed to eliminate all regurgitant gaps, we quantified the percent difference of the gap size relative to the annular orifice area. From those numbers, it appears the Classic device was most effective in reestablishing leaflet coaptation, whereas the Contour device was least effective. That is, the Classic device required the least annular reduction (size 34) to establish full coaptation, whereas the Contour device required the most annular reduction (size 28).

To deepen our coaptation analyses, we next depict how device shape and size affect the ratio between the coaptation area and leaflet area. In other words, we quantify how much of the leaflet is being effectively used toward closure. Figure 4 shows these ratios for each device shape and size relative to the healthy baseline and the unrepaired disease case. We found that, for a given device size, the Classic produced the most coaptation area while the Physio produced the least. We also found that sizes 30 and smaller, regardless of shape, restored healthy levels of coaptation area.

Leaflet Motion

We also investigated post-repair leaflet motion. Here, we define end-systolic angle as the angle between the annular plane and each leaflet at end-systole (Figure 5, *A*). Figure 5, *B*, shows the end-systolic angle for each leaflet and each repair case. Interestingly, device shape had a leaflet-dependent effect on leaflet motion. That is, for the anterior and posterior leaflets, we found that all devices led to a decrease in end-systolic angles relative to baseline conditions. In contrast, for the septal leaflet, most devices increased the end-systolic angle relative to the healthy baseline. Similarly, device size also had a leaflet-dependent impact. For the anterior leaflet, we found that decreasing device size led to decreasing end-systolic angle, whereas in the posterior leaflet, the end-systolic angle appeared independent of device size. Finally, for the septal leaflet, decreasing device size appeared to increase the end-systolic angle. To rank all devices, we summed the difference between the end-systolic angles between the healthy baseline and the repaired cases across all leaflets and sizes. Thereby, we found that the Contour device led to the smallest total differences in end-systolic angle whereas the Classic device led to the largest total differences in end-systolic angle (Table 2). We conducted a similar analysis for device size (Table 3). Here we found that—across leaflets and device shapes—increasing device size led to decreasing differences in end-systolic angle.

TABLE 1. Annuloplasty device specifications

Size	26	28	30	32	34	36
			Device area, mm^2			
Classic	409.40	464.46	536.54	594.72	666.28	743.13
Physio	486.45	557.78	624.17	715.02	806.15	882.55
MC3	426.30	480.25	570.66	638.75	969.04	777.43
Contour	453.43	476.00	578.34	652.91	726.01	827.05
			Device height, mm			
Classic	1.06	2.14	2.53	2.50	2.48	2.52
Physio	3.53	3.72	4.19	4.60	4.99	5.86
MC3	4.86	4.85	5.45	5.48	6.70	6.96
Contour	7.60	7.08	8.31	8.11	8.93	10.07

Note that the area of the healthy tricuspid annulus of the Texas TriValve is 564.57 mm^2 at end-diastole and 396.87 mm^2 at end-systole, whereas the area of the unrepaired diseased valve is 917.6 mm^2 at both end-diastole and end-systole. The height of the healthy tricuspid annulus is 7.14 mm at end-systole whereas the height of the unrepaired diseased valve is 6.29 mm at end-systole.

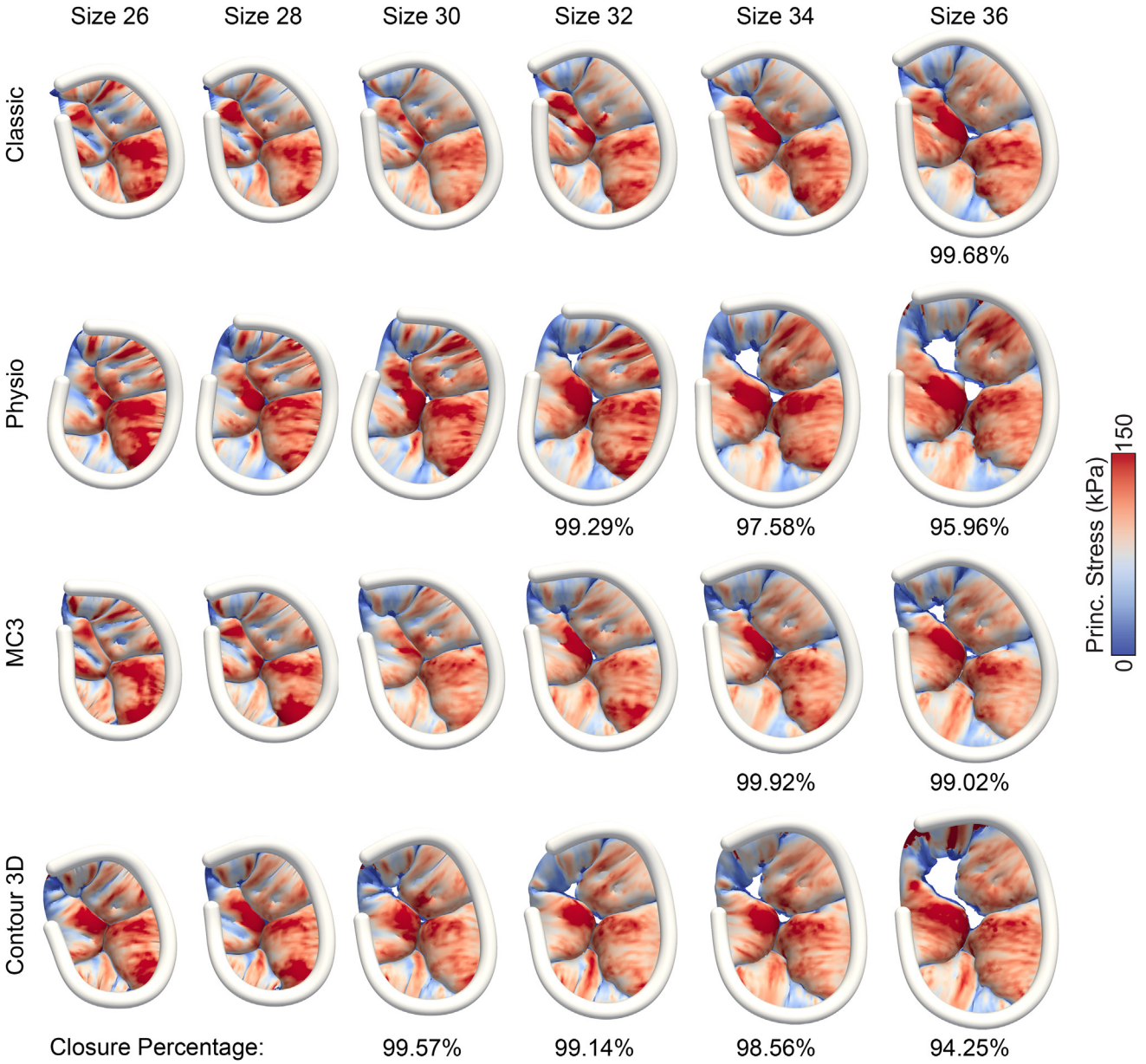

FIGURE 3. Atrial view of all repair cases overlaid with maximum principal Cauchy stress. Closure percentage, ie, regurgitant gap size relative to total orifice area, is reported below any repair simulation with a value less than 100%.

Leaflet Stress

Additionally, we investigated the device-induced stress in each leaflet. Figure 5, *C*, shows the average maximum principal Cauchy stress across each leaflet center, whereas Figure 5, *D*, shows regions where those stresses were averaged. Here, again, we found that the impact of device shape and size was leaflet-dependent. For the anterior leaflet, we found that all devices led to an increase in leaflet stress relative to the unrepaired case and could not restore healthy baseline stress. In contrast, in both the posterior and septal leaflets, all devices lead to a decrease in leaflet stress relative to the unrepaired case and trended toward restoring healthy baseline stress. As for the impact of device size, we found that, for the anterior leaflet, stress was independent of device size. In contrast, in both the posterior and septal leaflets, stress decreased with decreasing device size toward healthy baseline conditions. Again, to rank devices, we summed the difference between stress in the healthy and the repaired valves across all leaflets and sizes. Thereby, we found that the Classic device led to the smallest total differences in stress

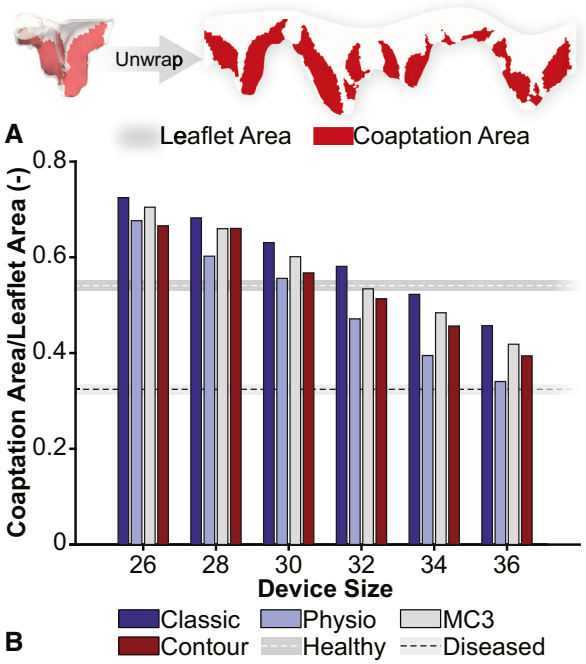

FIGURE 4. Smaller annuloplasty rings restore leaflet coaptation. A, We quantify leaflet coaptation as the sum of areas of all shell elements in contact at end-systole, depicted here in *red* and projected on a two-dimensional representation of the leaflet surface. B, All tricuspid valve annuloplasty devices restore healthy coaptation area for size 30 and smaller.

whereas the Physio device led to the largest total differences in stress (Table 2). We conducted a similar analysis for device size (Table 3). Here we found that—across leaflets and device shapes—increasing device size led to increasing differences in leaflet stress.

Chordal Forces

In our final analysis, we investigated the impact of device shape and size on chordal forces. Figure 6 shows the total sum of all chordal forces in the apical direction. Here we found that chordal forces depended on both device shape and size. Of the 4 devices, the Contour induced the largest forces. Conversely, the Classic induced the smallest chordal forces, approximating those forces of the healthy baseline. We also found that chordal forces increased with increasing device size, much faster so for the Contour and the Physio device than for the other 2 devices.

COMMENT

In this study, summarized in Figure 7, we used our previously developed subject-specific finite element model of the human tricuspid valve to investigate the impact of annuloplasty device shape and size on valve mechanics. By implanting 4 different devices (ie, shapes) of 6 different sizes in our virtual patient, we showed that the choice of device shape and size significantly impacts valve mechanics.

Impact of Device Shape

Specifically, we found that device shape impacts all measures of valve mechanics, including its coaptation area, leaflet motion, leaflet stress, and chordal forces. For example, the Classic produced the most coaptation area for a given size and the Physio the least. This trend correlates with these devices' "true" size. That is, the Classic device has the smallest "true" inscribed area, while the Physio has the largest.[20] The impact of device shape on leaflet motion and leaflet stress was more complex in that it was leaflet-dependent. However, overall, we found that the Contour device led to the smallest overall deviations from healthy end-systolic angles, whereas the Classic device led to the largest deviations. Interestingly, this trend correlates with these devices' degree of "contour" or height. Specifically, the Classic is the flattest of the devices with a near-zero height, whereas the Physio and MC3 are mid-high, and the Contour has the most height. Thus, it appears that the three-dimensional profile of the devices allows for more physiological leaflet motion. We also found that the Classic device led to the smallest overall deviations of stress from the healthy case while the Physio device led to the largest deviation in stress. Thus, device height appears negatively correlated with achieving healthy leaflet stress. Increased stress also induced larger chordal forces so that the Classic led to the most physiological sub-annular mechanics, whereas the Contour led to the largest chordal forces. This is somewhat contradictory with findings on the mitral valve, where it was suggested that increased "saddle" or profile height leads to lower stress.[21] Overall, it appears that there is no perfect device solution. Although the low-profile Classic device most effectively reestablished coaptation area, healthy leaflet stress, and chordal forces, it disrupted leaflet motion most. Especially on the septal leaflet, it led to early coaptation well below the annular plane. In contrast, the Contour device was most effective in reestablishing healthy leaflet motion but appeared suboptimal in creating coaptation area, healthy leaflet stress, and normal chordal forces.

Shape Recommendation for Our Virtual Patient

For our one virtual patient, we recommend the Classic device. It outperformed the other 3 devices in 3 critical measures of valve mechanics: coaptation area, leaflet stress, and chordal forces. It was beat out only in its ability to restore healthy leaflet motion. However, since the impact of changes to leaflet motion is currently unknown, we weigh its importance for the time being as low. This comes somewhat as a surprise given that the Classic device, as the name suggests, is the oldest and presumably least evolved of the 4. It appears that here the adage "oldie but goodie" applies.

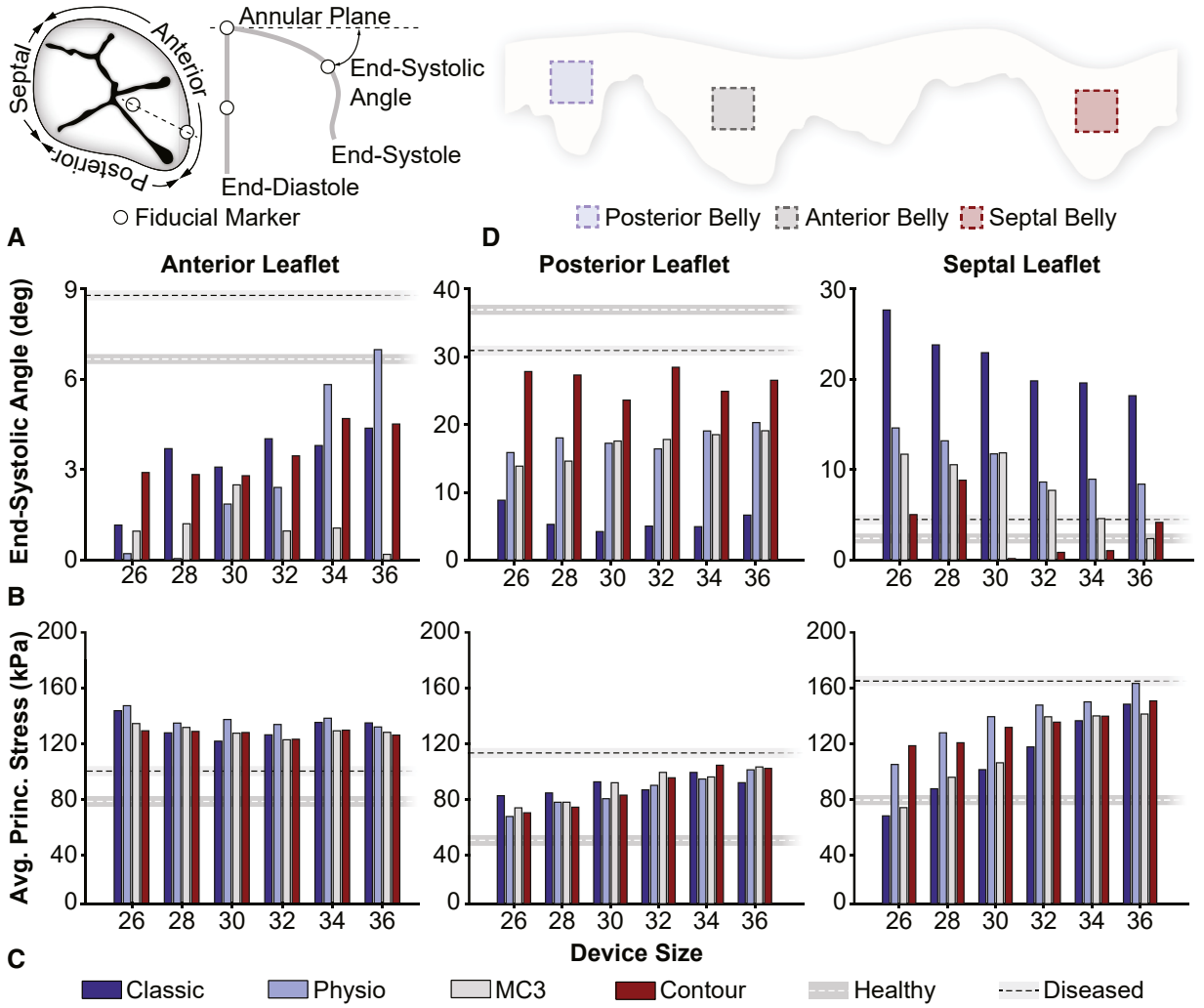

FIGURE 5. Tricuspid annuloplasty devices impact leaflet motion and stress. A, Here, we define the end-systolic angle for each leaflet as the angle made by a virtual fiducial marker and the annular plane at end-systole. B, Tricuspid annuloplasty devices fail to restore healthy leaflet motion. C, Tricuspid valve annuloplasty devices have a leaflet-dependent impact on stress. D, Please note, we average maximum principal Cauchy stresses in the belly region of each valve leaflet, indicated by the shaded regions on a two-dimensional representation of the leaflet surface.

Impact of Device Size

We also found that device size impacts all measures of valve mechanics. For example, we found that the coaptation area increased with decreasing device size. The impact of device size on leaflet motion was more complex. Here, we found that size had a leaflet-dependent impact. Increasing size led to larger end-systolic angles in the anterior leaflet relative to the healthy baseline while being the opposite in the septal leaflet and having no effect in the posterior leaflet. Across leaflets and device shapes, we found that increasing device size led to smaller deviations in end-systolic angle from the healthy baseline. The impact of device size on leaflet stress was similarly complex, yet with different trends. Here increasing device size led to increasing leaflet stress in both the posterior and the septal leaflets relative to the healthy baseline but had minimal impact on stress in the anterior leaflet. This finding for the anterior leaflet was somewhat surprising as others have argued that, in the spirit of Laplace's law, increasing annular size, ie, radius, would globally lead to larger stress.[22,23] However, it appears that for the anterior leaflet the kinematic constraints due to chordal attachment and contact negate the simplifying assumptions of Laplace's law. Across leaflets and device shapes, we found that increasing device size increased overall leaflet stress. This trend coincided with the impact of device size on chordal forces. That is, increasing device size also increased the chordal forces. Overall, as for the device shape, there is no perfect device size. Although smaller devices maximize the coaptation area and minimize leaflet stress and chordal forces, they

TABLE 2. Total device-induced change in end-systolic angle and stress for each device shape

Shape	Σ Angle, deg	Σ Stress, kPa
Classic	324.04	759.5
Physio	189.07	918.5
MC3	187.65	773.5
Contour	97.61	841.6

For end-systolic angle and stress, we summed the differences between the healthy baseline and each repair case across all leaflets and device sizes. Note, we report stress as the average maximum principal Cauchy stress across each leaflet center.

led to abnormal leaflet motion. Conversely, larger devices, while normalizing leaflet motion, limit the coaptation area and induce larger leaflet stress and chordal forces.

Size Recommendation for Our Virtual Patient

Annuloplasty device sizing, both on the tricuspid and the mitral valve, may not always be grounded in science.[24] Here we found that a device of size 30 for the Classic device was sufficiently small to restore normal coaptation area while providing a good trade-off against the disruption of leaflet end-systolic angle and leaflet stress. Without knowledge about the relative importance of the coaptation area, end-systolic angle, leaflet stress, and chordal forces, we recommend a size 30 to our patient. Thus, we don't choose an excessive undersizing strategy as others have done.[10,11] This choice is also supported by our previous work in sheep in which we found that excessive undersizing (ie, choosing devices smaller than 30) may negatively impact right ventricular function.[25] Future studies may find that increased leaflet stress may be an important factor in leaflet remodeling and may contribute to long-term repair failure, in which case we would re-evaluate our recommendation.[16,26] That is, we would recommend a smaller size that reduces remodeling-inducing leaflet stress. Please note that we found the impact of device size to be shape-dependent. Thus, our size recommendation should be understood to depend on our device choice.

TABLE 3. Total device-induced change in end-systolic angle and stress for each device size

Size	Σ Angle, deg	Σ Stress, kPa
26	152.14	414.6
28	148.13	436.2
30	143.04	507.9
32	126.30	584.5
34	118.83	659.8
36	109.92	690.2

For end-systolic angle and stress, we summed the differences between the healthy baseline and each repair case across all leaflets and device shapes. Note, we report stress as the average maximum principal Cauchy stress across each leaflet center.

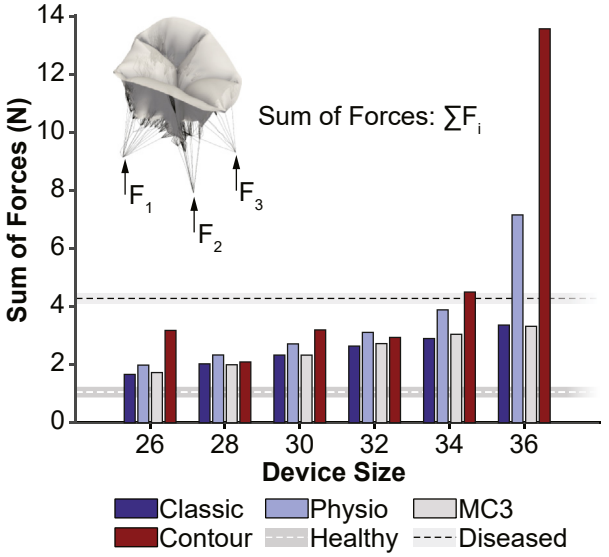

FIGURE 6. Tricuspid valve annuloplasty devices alter chordal forces and—dependent on device shape and size—can approximate the healthy baseline

Limitations

Our study is subject to several limitations. Most importantly, this is not a population study but a case study on a single virtual patient. Thus, our findings cannot be extrapolated to other patients and should be interpreted carefully. Also, importantly, we have ignored hemodynamics. Our current model only considers the hyperelastic quasi-static response of the tricuspid valve. For example, we have ignored that decreasing device size increases the pressure gradient across the valve. We want to note, however, that we have previously shown in sheep that even dramatic annular cinching leads to minor gradients that are not clinically significant.[27] In future refinements of our virtual valve model, we plan to incorporate fluid dynamics to capture blood flow across the valve and better quantify repair outcomes. We also plan to build many more patient specific valves using automatic segmentation and material property estimation of non-invasive patient imaging data. Additionally, only one disease pathology reflecting pulmonary arterial hypertension-induced functional tricuspid regurgitation was considered in this study. However, our valve model is flexible to allow for investigations of other disease pathologies which present through changes of valve geometry and/or transvalvular pressure which opens opportunities for future clinically-relevant work.

CONCLUSIONS

Based on analyses of the coaptation area, leaflet motion, leaflet stress, and chordal forces, we found that device shape and size have a significant impact on valve mechanics. Further, we recommend that our virtual patient be treated

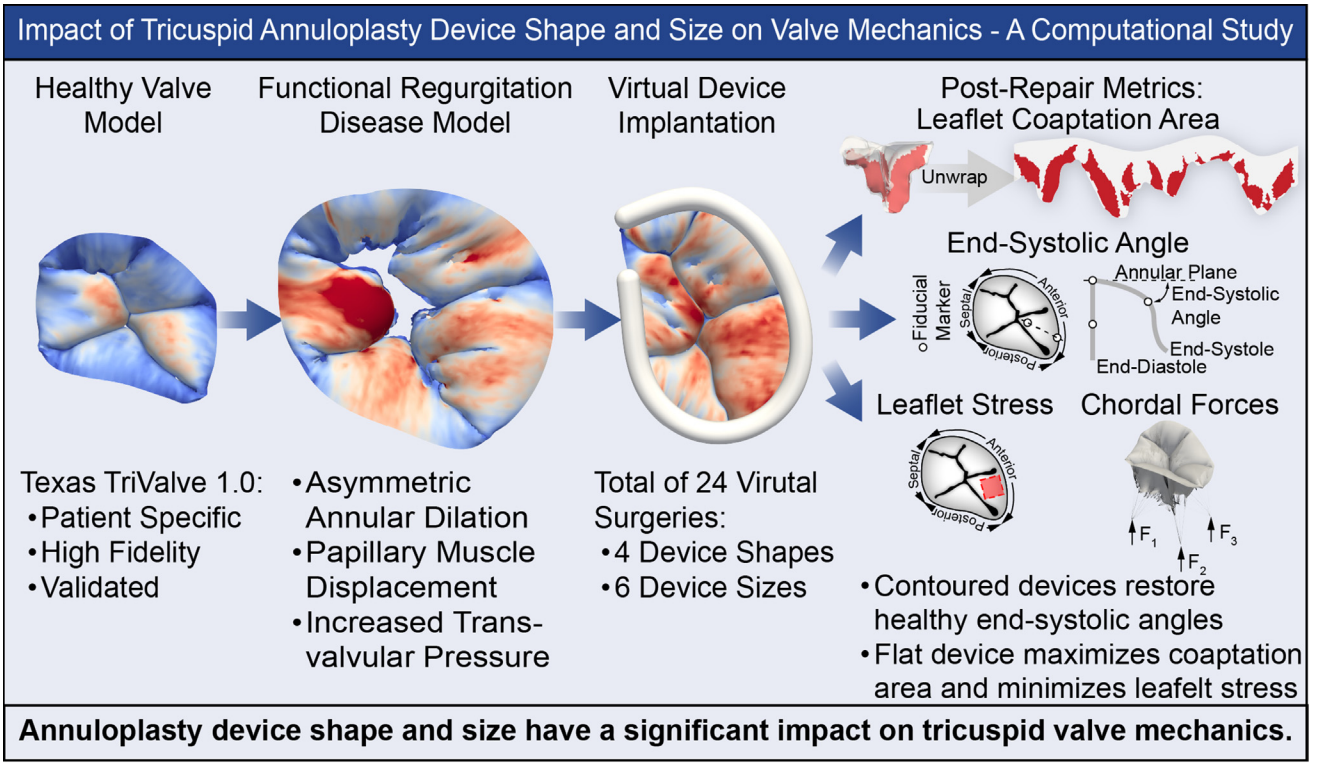

FIGURE 7. Overview of the healthy, diseased, and repaired tricuspid valve models used in this study, in addition to the key take-home messages.

with a Classic device of size 30. Importantly, this is a case study, and our recommendation cannot and should not be extrapolated to other patients or patient populations. More models like ours may allow in the future to understand subject-specific factors that render one device or size more optimal than others.

Conflict of Interest Statement

M.K.R. has a speaking agreement with Edwards Lifesciences. All other authors reported no conflicts of interest.

The *Journal* policy requires editors and reviewers to disclose conflicts of interest and to decline handling or reviewing manuscripts for which they may have a conflict of interest. The editors and reviewers of this article have no conflicts of interest.

References

1. Nath J, Foster E, Heidenreich PA. Impact of tricuspid regurgitation on long-term survival. *J Am Coll Cardiol*. 2004;43:405-9. https://doi.org/10.1016/j.jacc.2003.09.036
2. Rogers JH, Bolling SF. The tricuspid valve: current perspective and evolving management of tricuspid regurgitation. *Circulation*. 2009;119:2718-25.
3. Dreyfus GD, Martin RP, Chan KMJ, Dulguerov F, Alexandrescu C. Functional tricuspid regurgitation: a need to revise our understanding. *J Am Coll Cardiol*. 2015;65:2331-6.
4. Rod'es-Cabau J, Taramasso M, O'Gara PT. Diagnosis and treatment of tricuspid valve disease: current and future perspectives. *Lancet*. 2016;388:2431-42.
5. Taramasso M, Calen C, Guidotti A, Kuwata S, Biefer HRC, Nietlispach F, et al. Management of tricuspid regurgitation: the role of transcatheter therapies. *Intervent Cardiol*. 2017;12:51-5.
6. Navia JL, Nowicki ER, Blackstone EH, Brozzi NA, Nento DE, Atik FA, et al. Surgical management of secondary tricuspid valve regurgitation: annulus, commissure, or leaflet procedure? *J Thorac Cardiovasc Surg*. 2010;139:1473-82.e5. https://doi.org/10.1016/j.jtcvs.2010.02.046
7. Nosair A, Elkahely M, Nasr S, Alkady H. Tricuspid three-dimensional ring versus fashioned flexible band annuloplasty in management of functional tricuspid valve regurge: comparative long term study. *Cardiothorac Surg*. 2020;28:13. https://doi.org/10.1186/s43057-020-00023-2
8. Huffman LC, Nelson JS, Lehman AN, Krajacic MC, Bolling SF. Identical tricuspid ring sizing in simultaneous functional tricuspid and mitral valve repair: a simple and effective strategy. *J Thorac Cardiovasc Surg*. 2014;147:611-4.
9. Teman NR, Huffman LC, Krajacic M, Pagani FD, Haft JW, Bolling SF. "Prophylactic" tricuspid repair for functional tricuspid regurgitation. *Ann Thorac Surg*. 2014;97:1520-4.
10. Ghoreishi M, Brown JM, Stauffer CE, Young CA, Byron MJ, Griffith BP, et al. Undersized tricuspid annuloplasty rings optimally treat functional tricuspid regurgitation. *Ann Thorac Surg*. 2011;92:89-96.
11. Maghami S, Ghoreishi M, Foster N, Dawood MY, Hobbs GR, Stafford P, et al. Undersized rigid nonplanar annuloplasty: the key to effective and durable repair of functional tricuspid regurgitation. *Ann Thorac Surg*. 2016;102:735-42.
12. Taramasso M, Vanermen H, Maisano F, Guidotti A, La Canna G, Alfieri O. The growing clinical importance of secondary tricuspid regurgitation. *J Am Coll Cardiol*. 2012;59:703-10.

13. Algarni KD, Alfonso J, Pragliola C, Kheirallah H, Adam A, Arafat AA. Long-term outcomes of tricuspid valve repair: the influence of the annuloplasty prosthesis. *Ann Thorac Surg*. 2021;112:1493-500.
14. Mathur M, Meador WD, Malinowski M, Jazwiec T, Timek TA, Rausch MK. Texas TriValve 1.0: a reverse-engineered, open model of the human tricuspid valve. *Engin Comput*. 2022;38:3835-48. https://doi.org/10.1007/s00366-022-01659-w
15. Ring L, Rana BS, Kydd A, Boyd J, Parker K, Rusk RA. Dynamics of the tricuspid valve annulus in normal and dilated right hearts: a three-dimensional transoesophageal echocardiography study. *Eur Heart J*. 2012;13:756-62.
16. Meador WD, Mathur M, Sugerman GP, Malinowski M, Jazwiec T, Wang X, et al. The tricuspid valve also maladapts as shown in sheep with biventricular heart failure. *Elife*. 2020;9:e63855. https://doi.org/10.7554/eLife.63855
17. Spinner EM, Lerakis S, Higginson J, Pernetz M, Howell S, Veledar E, et al. Correlates of tricuspid regurgitation as determined by 3D echocardiography: pulmonary arterial pressure, ventricle geometry, annular dilatation, and papillary muscle displacement. *Circulation*. 2012;5:43-50. https://doi.org/10.1161/CIRCIMAGING.111.965707
18. Nickenig G, Kowalski M, Hausleiter J, Braun D, Schofer J, Yzeiraj E, et al. Transcatheter treatment of severe tricuspid regurgitation with the edge-to-edge MitraClip technique. *Circulation*. 2017;135:1802-14.
19. Gaidulis G, Padala M. Computational modeling of the subject-specific effects of annuloplasty ring sizing on the mitral valve to repair functional mitral regurgitation. *Ann Biomed Eng*. 2023;51:1984-2000. https://doi.org/10.1007/s10439-023-03219-9
20. Mathur M, Malinowski M, Timek TA, Rausch MK. Tricuspid annuloplasty rings: a quantitative comparison of size, nonplanar shape, and stiffness. *Ann Thorac Surg*. 2020;110:1605-14.
21. Salgo IS, Gorman JH, Gorman RC, Jackson BM, Bowen FW, Plappert T, et al. Effect of annular shape on leaflet curvature in reducing mitral leaflet stress. *Circulation*. 2002;106:711-7.
22. Arts T, Meerbaum S, Reneman R, Corday E. Stresses in the closed mitral valve: a model study. *J Biomech*. 1983;16:539-47. https://doi.org/10.1016/0021-9290(83)90068-4
23. Tibayan FA, Rodriguez F, Langer F, Zasio MK, Bailey L, Liang D, et al. Increases in mitral leaflet radii of curvature with chronic ischemic mitral regurgitation. *J Heart Valve Dis*. 2004;13:772-8.
24. Bothe W, Miller DC, Doenst T. Sizing for mitral annuloplasty: where does science stop and voodoo begin? *Ann Thorac Surg*. 2013;95:1475-83.
25. Jazwiec T, Malinowski M, Ferguson H, Wodarek J, Quay N, Bush J, et al. Effect of variable annular reduction on functional tricuspid regurgitation and right ventricular dynamics in an ovine model of tachycardia induced cardiomyopathy. *J Thorac Cardiovasc Surg*. 2021;161:e277-86.
26. Rausch MK, Tibayan FA, Miller DC, Kuhl E. Evidence of adaptive mitral leaflet growth. *J Mech Behav Biomed Mater*. 2012;15:208-17. https://doi.org/10.1016/j.jmbbm.2012.07.001
27. Mathur M, Meador WD, Jazwiec T, Malinowski M, Timek TA, Rausch MK. The effect of downsizing on the normal tricuspid annulus. *Ann Biomed Eng*. 2020;48:655-68. https://doi.org/10.1007/s10439-019-02387-x

Key Words: tricuspid valve, functional regurgitation, annuloplasty, repair, virtual surgery

APPENDIX E1. BRIEF DESCRIPTION OF THE TEXAS TriValve 1.0

We built this model of the human tricuspid valve from a donated healthy heart that was rejected from implantation. First, we used an organ-preservation system that perfused and paced the beating heart and recreated a realistic hemodynamic environment for the tricuspid valve. In this system, we measured transvalvular pressure, annular dynamics, and leaflet motion. After collecting these data, we excised the tricuspid valve and conducted in vivo and in vitro geometric and material characterizations of the valve leaflets and chordae tendineae. That is, we first took images of the flattened valve leaflets to quantify their shape, which we then nonrigidly transformed onto the shape of the in vivo annulus. Next, we quantified chordal insertion sites from those same images and marked them in our geometric valve model. Then, we mechanically interrogated each valve leaflet and each leaflet's chordae tendineae using biaxial and uniaxial extension, respectively. We cast these data into the form of a Fung-type constitutive model[E1,E2] and the Ogden material model,[E3] again, respectively. We assumed both materials to behave quasi-incompressibly. In addition, we measured the thickness of valve leaflets and chordae, which we assigned to the geometric representation of the valve. Finally, we discretized leaflets using linear quadrilateral shell finite elements (Abaqus element S4R), while we discretized the chordae using three-dimensional linear multi-segmented truss elements (Abaqus element T3D2).[E4] We validated our model against echo-based measurements taken in the organ-preservation system.

APPENDIX E2. SIMULATION DETAILS

The virtual repairs themselves were conducted as follows: First, we identified for each device an orientation that best fit the diseased shape of the annulus under the constraint that the anterior portion of the septal annulus remained free. Next, we displaced all finite element nodes along the tricuspid annulus toward the closest point along the device, which we modeled as a rigid body owing to the devices' high stiffness. In addition, we displaced the free nodes of the anterior portion of the septal annulus along a smooth line connecting the 2 ends of the annuloplasty devices. Finally, after the annuloplasty devices were virtually implanted in the diseased valve, we applied the transvalvular pressure gradient to the ventricular surface of each leaflet to quasi-statically simulate valve closure. All simulations were conducted in Abaqus/Explicit 2020 (Dassault Systèmes, Vélizy-Villacoublay, France) on one Intel Xeon Platinum 8160 "Skylake" node at the Texas Advanced Computing Center. We discretized the leaflets with 8819 elements and the chordae with 3002 elements. In addition, we used uniform mass scaling to ensure a minimum stable time increment of 1×10^{-6} seconds. Moreover, we used Abaqus' general contact scheme with the frictional penalty set to 0.1[E5] to enforce contact between the leaflets.

E-References

E1. Kamensky D, Xu F, Lee CH, Yan J, Bazilevs Y, Hsu MC. A contact formulation based on a volumetric potential: application to isogeometric simulations of atrioventricular valves. *Comput Methods Appl Mech Eng*. 2018;330:522-46. https://doi.org/10.1016/j.cma.2017.11.007

E2. Meador WD, Mathur M, Sugerman GP, Jazwiec T, Malinowski M, Bersi MR, et al. A detailed mechanical and microstructural analysis of ovine tricuspid valve leaflets. *Acta Biomater*. 2020;102:100-3. https://doi.org/10.1016/j.actbio.2019.11.039

E3. Smith KJ, Mathur M, Meador WD, Phillips-Garcia B, Sugerman GP, Menta AK, et al. Tricuspid chordae tendineae mechanics: insertion site, leaflet, and size-specific analysis and constitutive modelling. *Exp Mech*. 2021;61:19-29. https://doi.org/10.1007/s11340-020-00594-5

E4. Lee CH, Rabbah JP, Yoganathan AP, Gorman RC, Gorman JH III, Sacks MS. On the effects of leaflet microstructure and constitutive model on the closing behavior of the mitral valve. *Biomech Model Mechanobiol*. 2015;14:1281-302. https://doi.org/10.1007/s10237-015-0674-0

E5. Pasta S, Catalano C, Cannata S, Guccione JM, Gandolfo C. Numerical simulation of transcatheter mitral valve replacement: the dynamic implication of LVOT obstruction in the valve-in-ring case. *J Biomech*. 2022;144:111337. https://doi.org/10.1016/j.jbiomech.2022.111337